HP-6

# 3-D Steady-State Eddy Current Damping and Stiffness Terms for a Finite Thickness Conductive Plate

Subhra Paul, Jason Wright and Jonathan Z. Bird

Laboratory for Electromechanical Energy Conversion and Control University of North Carolina at Charlotte, NC 28223 USA

In this paper the 3-D forces created by induced eddy currents in a conductive plate of finite thickness are derived using the concept of magnetic charge and energy. By using this approach the exact steady-state based eddy-current damping and stiffness matrices for an arbitrary magnetic source moving above a conductive plate are derived. The damping and stiffness terms caused by both angular and spatial motion are accounted for. The presented equations can be utilized to create a linear state-space eddy current force model.

Index Terms-Eddy currents, Halbach rotor, stiffness, damping

#### I. Introduction

N order to accurately model and control the dynamic motion Lof electromechanical devices subjected to eddy current forces the precise calculation of the eddy current force is important. A range of authors have utilized analytic field based models to study conductive plate eddy current electromechanical dynamics. For instance, Davis and Yoshida utilized field based thin-sheet approximations to study the eddy current force dynamics for a long wire and a thin coil moving above a continuously uniform conductive plate [1-2] and Langerholc analytically studied vertical motion for a coil moving above a conductive half-space [3]. Other authors have calculated damping equations for a limited range of directions [3-8]. In this paper damping is defined as the partial derivative of force with respect to velocity  $\partial F / \partial v$  and not F/v as used by some authors [6]. For control purposes it would be particularly useful if the eddy current forces could be derived in a form that can be utilized within the linear statespace framework [9]. In order to do this the eddy current forces need to be linearized and the eddy current damping and stiffness equations need to be determined. Ooi appears to be one of the only authors to derive complete damping and stiffness matrices for a conductive plate. However in this treatment approximate circuit based modeling was used [10].

In this paper the exact 3-D steady-state eddy current damping and stiffness equations are derived within the non-conductive region and expressed in a form that can be utilized in a linearized state-space formulation. In many electromechanical devices the mechanical time constant is much larger than the electrical time constant and therefore the use of steady-state eddy current force equations with a dynamic mechanical model will lead to accurate electromechanical results [7-8].

## II. 3-D EDDY CURRENT FIELD MODEL

It is well known that when modeling eddy current problems with conductive plates the surrounding non-conductive regions can be modeled using a magnetic scalar potential,  $\phi$ , and the conductive regions can be modeled using the magnetic vector potential, **A** [11]. When the source field penetrates into the conductive plate it induces current within the plate, via Faraday's law, that will result in a "reflected"

eddy current field [3, 8, 12-13]. This reflected field then interacts with the source field to create force. The nonconductive regions between the source and the conductive plate are then governed by the magnetostatic field equations. Due to the solenoidal nature of magnetic fields  $\nabla \cdot \mathbf{B} = 0$  the forces within the magnetostatic field region cannot be stable [14]. However, it is well known that eddy currents induced in a conductive plate can indeed create stability [15-16]. This is possible because the eddy currents within a conductive plate are not governed by the magnetostatic equations. Nevertheless, between the plate and the source the reflected field must always satisfy the magnetostatic equations. It can therefore be concluded that at any instant in time the forces created by the magnetic fields within the non-conductive region are unstable; however, the eddy currents if properly configured using the right geometric design react to the motion of the source in a way that stabilizes the system without active control.

If the reflected field is modeled using the magnetic scalar potential,  $\phi^r$ , and the source field is modeled using a fictitious surface distribution of magnetic charge,  $\rho_{ms}$ , then the energy associated with the surface charge distribution interacting with the reflected field will be [17]

$$U_m = \frac{1}{2} \int_{S} \rho_{ms}^* \phi^r dS \tag{1}$$

The star superscript denotes complex conjugation. Only real part of (1) should be considered for energy calculation. As force within a magnetostatic region is defined as

$$\mathbf{F} = -\nabla U_m \Big|_{\rho_{ms} = \text{constant}} \tag{2}$$

then holding  $\rho_{ms}$  constant the force in a magnetostatic region is

$$\mathbf{F} = -\frac{1}{2} \int_{S} \rho_{ms}^* \nabla \phi^r dS \ . \tag{3}$$

As the scalar potential and flux density are related by

$$\mathbf{B}^r = -\mu_0 \nabla \phi^r \tag{4}$$

the force can be written as [18-19]

$$\mathbf{F} = \frac{1}{2\mu_0} \int_{S} \rho_{ms}^* \mathbf{B}^r dS . \tag{5}$$

The external field created by a magnetic source can be reproduced using an equivalent fictitious magnetic charge HP-6 2

sheet [8, 20]. In this paper the charge sheet is located a distance g above a finite thickness conductive plate. The problem formulation is represented as shown in Fig. 1. It is assumed that the plate width, w, and length, l, is sufficiently large that the eddy current fields and source fields are zero at the plate edges. In order to correctly model the external field the magnetic charge distribution on the planar sheet must satisfy [20]

$$\rho_{ms}(x,z) = 2B_y^s(x,g,z) \tag{6}$$

where  $B_y^s$  is the normal component of the source field at height y=g. Substituting (6) into (5) gives the force in Maxwell stress tensor form:

$$\mathbf{F} = \frac{1}{\mu_0} \int_{-l/2 - w/2}^{l/2} \int_{-w/2}^{w/2} B_y^s(x, g, z)^* \mathbf{B}^r(x, g, z) dx dz$$
 (7)

It is not the typical form seen when using shear stress equations in that the field contributions from the source and the eddy currents are delineated. The reflected steady-state eddy current field created above the conductive plate is given by [8, 13]

$$\mathbf{B}^{r}(x,y,z,t) = -j \sum_{m=-\infty}^{\infty} \sum_{n=-\infty}^{\infty} S_{mn} R_{mn} [\xi_{m} \hat{x} + j\kappa_{mn} \hat{y} + k_{n} \hat{z}]$$

$$\times \frac{1}{\kappa} e^{-\kappa_{mn}(y+g)} e^{j\xi_{m} x} e^{jk_{n} z} e^{-jP\omega_{m} t}$$
(8)

where  $R_{mn}$  is the reflection coefficient

$$R_{mn} = \frac{\mu_0 \sigma \tau_{mn}}{\xi_m^2 + k_n^2 + \gamma_{mn}^2 + 2\kappa_{mn}\beta_{mn} \coth(\beta_{mn}h)}$$
(9)

and

$$\xi_m = 2\pi m/l \tag{10}$$

$$k_n = 2\pi n/w \tag{11}$$

$$\beta_{mn}^2 = \lambda^2 + \gamma_{mn}^2 \tag{12}$$

$$\lambda = -0.5v_{y}\mu_{0}\sigma\tag{13}$$

$$\gamma_{mn}^2 = \kappa_{mn}^2 - j\mu_0 \sigma (Pw_m + \xi_m v_x + k_n v_z) \tag{14}$$

$$\kappa_{mn}^2 = \xi_m^2 + k_n^2 \tag{15}$$

(17)

$$\tau_{mn} = \kappa_{mn} v_y + j(Pw_m + \xi_m v_x + k_n v_z) \tag{16}$$

The term  $S_{mn}$  in (8) is the source Fourier harmonic component. In this paper the source field is assumed to be created by a Halbach rotor that is rotating at angular velocity  $\omega_m$ . The  $B_y$  component of the source field for a Halbach rotor can be accurately modeled in 3-D by [8, 20]

$$B_{y}^{so}(x,y,z,t) = \frac{B_{r} r_{o} e^{-jP\omega_{m}t}}{2\pi} \int_{0}^{2\pi} \int_{-w_{o}/2}^{w_{o}/2} \frac{e^{jP\theta_{o}}}{R^{3}} (y - y_{c} - r_{o} \sin \theta_{o}) dz_{o} d\theta_{o}$$

where  $B_r = \frac{2B_{res}P(1+\mu_r)(r_i^{P+1}-r_o^{P+1})r_o^{2P}}{(1+P)[(1-\mu_s)^2r_s^{2P}-(1+\mu_s)^2r_s^{2P}]}\frac{1}{r_s^{P+1}}$  (18)

$$R = [(x - x_c - r_0 \cos \theta_0)^2 + (y - y_c - r_0 \sin \theta_0)^2 + (z - z_c - z_0)^2]^{1/2}$$
 (19)

The Halbach rotor parameters are defined in Table 1. The Halbach rotor is assumed to be centered at  $(x_c, y_c, z_c)$ . The complex exponential term in (17) is used to model the field

rotation of the Halbach rotor in steady-state [8, 13]. In order to couple the source field with the conductive plate and for term-by-term mode matching the source must be put into Fourier harmonic form. Defining the Fourier harmonic field at y=g as

$$B_y^s(x,g,z,t) = \sum_{m=-\infty}^{\infty} \sum_{n=-\infty}^{\infty} S_{mn} e^{j\xi_m x} e^{jk_n z} e^{-jP\omega_m t}$$
 (20)

then the harmonic terms in (20) are determined from (17) by evaluating [8, 20]

$$S_{mn} = \frac{1}{lw} \int_{-w/2}^{w/2} \int_{-l/2}^{l/2} B_y^{so}(x, g, z, t) e^{-j\xi_m x} e^{-jk_n z} dx dz$$
 (21)

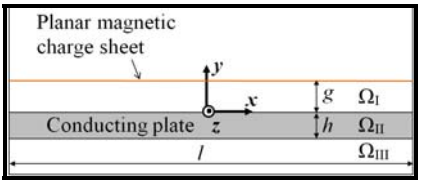


Fig. 1. An *x*-*y* view of the problem region with magnetic charge sheet located a distance *g* above a conductive plate. The plate has length *l* and width *w*.

 $\label{eq:table I} \textbf{TABLE I} \\ \textbf{Halbach Rotor and Conductive Plate Parameters} \\$ 

	Quantity	Value	Unit
Magnetic rotor	Outer radius, $r_o$	26	mm
	Inner radius, $r_i$	9.6	mm
	Width, $w_o$	52	mm
	Residual flux density, $B_{res}$	1.42	T
	Relative permeability, $\mu_{\rm r}$	1.108	-
	Pole pairs, P	2	-
Conductive plate	Conductivity, $\sigma$	2.459×10 <sup>7</sup>	S/m
	Width, $l_z$	150	mm
	Length, $l_x$	250	mm
	Thickness, h	6.3	mm
	Air-gap, g	5	mm

## III. STEADY-STATE FORCE AND TORQUE

Substituting (8) and (20) into (7) gives the 3-D eddy current force

$$\mathbf{F} = wl \operatorname{Re} \left\{ \sum_{m=-\infty}^{\infty} \sum_{n=-\infty}^{\infty} B_{mn}^{s} R_{mn} \left[ \frac{j\xi_{m}}{\kappa_{mn}} \hat{x} - \hat{y} + \frac{jk_{n}}{\kappa_{mn}} \hat{z} \right] \right\}$$
(22)

where 
$$B_{mn}^{s} = \frac{1}{\mu_0} |S_{mn}|^2 e^{-2\kappa_{mn}g}$$
 (23)

Equations of the same form have previously been derived [3, 12] but in these derivations the reflection function only contained the  $v_x$  term. The eddy current torque created by the rotation of the Halbach rotor is [8]

$$T_{em} = -\frac{\partial U_m}{\partial \theta_m} \bigg|_{\rho_{ms} = \text{constant}} = wl \operatorname{Re} \left\{ \sum_{m=-\infty}^{\infty} \sum_{n=-\infty}^{\infty} B_{mn}^s R_{mn} \frac{-jP}{\kappa_{mn}} \right\}$$
(24)

where  $\theta_{m} = \omega_{m} t$  (25)

## IV. STEADY-STATE STIFFNESS TERMS

The stiffness constant is defined as the negative of the change in force with respect to displacement [19]. Therefore positive values indicate stability. The stiffness matrix for the force and torque components can be written as HP-6

$$[\mathbf{k}] = \begin{bmatrix} k_{xx} & \mathbf{k}_{xy} & k_{xz} & k_{x\theta} \\ \mathbf{k}_{xx} & k_{yy} & k_{yz} & k_{y\theta} \\ k_{zx} & k_{zy} & k_{zz} & k_{z\theta} \\ k_{x} & k_{y} & k_{z} & k_{\theta} \end{bmatrix} = - \begin{bmatrix} \frac{\partial F_{x}}{\partial x} & \frac{\partial F_{x}}{\partial y} & \frac{\partial F_{x}}{\partial z} & \frac{\partial F_{x}}{\partial \theta_{m}} \\ \frac{\partial F_{y}}{\partial x} & \frac{\partial F_{y}}{\partial y} & \frac{\partial F_{y}}{\partial z} & \frac{\partial F_{y}}{\partial \theta_{m}} \\ \frac{\partial F_{z}}{\partial x} & \frac{\partial F_{z}}{\partial y} & \frac{\partial F_{z}}{\partial z} & \frac{\partial F_{z}}{\partial \theta_{m}} \\ \frac{\partial F_{z}}{\partial x} & \frac{\partial F_{z}}{\partial y} & \frac{\partial F_{z}}{\partial z} & \frac{\partial F_{z}}{\partial \theta_{m}} \end{bmatrix}$$
 (26)

From (22) it can be seen that the spatial terms are no longer present. However, the stiffness can be calculated by utilizing the energy description given by (1). As in electrostatics when taking the derivative with position either the charge density function or the field function is held constant [17]. For instance using (1)  $\partial F_r / \partial y$  will be

$$\frac{\partial F_x}{\partial y} = -\frac{1}{2} \left[ \int_S \rho_{ms}^* \frac{\partial^2 \phi^r}{\partial x \partial y} dS \right]_0$$
 (27)

Utilizing this approach the off-diagonal terms in (26) are

$$k_{xy} = k_{yx} = wl \operatorname{Re} \left\{ \sum_{m=-\infty}^{\infty} \sum_{n=-\infty}^{\infty} j \xi_m B_{mn}^s R_{mn} \right\}$$
 (28)

$$k_{yz} = k_{zy} = wl \operatorname{Re} \left\{ \sum_{m=-\infty}^{\infty} \sum_{n=-\infty}^{\infty} j k_n B_{mn}^s R_{mn} \right\}$$
 (29)

$$k_{xz} = k_{zx} = wl \operatorname{Re} \left\{ \sum_{m=-\infty}^{\infty} \sum_{n=-\infty}^{\infty} \frac{\xi_m k_n}{\kappa_{mn}} B_{mn}^s R_{mn} \right\}$$
(30)

$$k_{x\theta} = k_{\theta x} = -wlP \operatorname{Re} \left\{ \sum_{m=-\infty}^{\infty} \sum_{n=-\infty}^{\infty} \frac{\xi_m}{\kappa_{mn}} B_{mn}^s R_{mn} \right\}$$
(31)

$$k_{y\theta} = k_{\theta y} = -wlP \operatorname{Re} \left\{ \sum_{m=-\infty}^{\infty} \sum_{n=-\infty}^{\infty} j B_{mn}^{s} R_{mn} \right\}$$
 (32)

$$k_{z\theta} = k_{\theta z} = -wlP \operatorname{Re} \left\{ \sum_{m=-\infty}^{\infty} \sum_{n=-\infty}^{\infty} \frac{k_n}{\kappa_{mn}} B_{mn}^s R_{mn} \right\}$$
(33)

while the diagonal terms in (26) are evaluated to be

$$k_{xx} = wl \operatorname{Re} \left\{ \sum_{m=-\infty}^{\infty} \sum_{n=-\infty}^{\infty} \frac{\xi_m^2}{\kappa_{mn}} B_{mn}^s R_{mn} \right\}$$
(34)

$$k_{yy} = -wl \operatorname{Re} \left\{ \sum_{m=-\infty}^{\infty} \sum_{n=-\infty}^{\infty} \kappa_{mn} B_{mn}^{s} R_{mn} \right\}$$
 (35)

$$k_{zz} = wl \operatorname{Re} \left\{ \sum_{m=-\infty}^{\infty} \sum_{n=-\infty}^{\infty} \frac{k_n^2}{\kappa_{mn}} B_{mn}^s R_{mn} \right\}$$
 (36)

$$k_{\theta} = wlP^2 \operatorname{Re} \left\{ \sum_{m=-\infty}^{\infty} \sum_{n=-\infty}^{\infty} \frac{1}{\kappa_{mn}} B_{mn}^s R_{mn} \right\}$$
 (37)

By thinking of the stiffness as being derived from energy it can be relatively easily understood that the off-diagonal terms must all be symmetric [10]. From (34)-(36) it can also be noted that

$$k_{xx} + k_{zz} + k_{yy} = 0 ag{38}$$

Therefore, the steady-state eddy current forces are solenoidal  $\nabla \cdot \mathbf{F} = 0$  (39)

In addition, as the stiffness matrix is diagonally symmetric

$$\nabla \times \mathbf{F} = 0 \tag{40}$$

## V. STEADY-STATE DAMPING TERMS

The damping coefficients are caused by the changes in the force and torque with respect to velocity and angular velocity. The damping coefficient matrix for the 3-D model is

$$[\mathbf{D}] = \begin{bmatrix} D_{xx} & D_{xy} & D_{xz} & D_{x\theta} \\ D_{yx} & D_{yy} & D_{yz} & D_{y\theta} \\ D_{zx} & D_{zy} & D_{zz} & D_{z\theta} \\ D_{x} & D_{y} & D_{z} & D_{\theta} \end{bmatrix} = - \begin{bmatrix} \frac{\partial F_{x}}{\partial v_{x}} & \frac{\partial F_{x}}{\partial v_{y}} & \frac{\partial F_{x}}{\partial v_{z}} & \frac{\partial F_{x}}{\partial \omega_{m}} \\ \frac{\partial F_{y}}{\partial v_{x}} & \frac{\partial F_{y}}{\partial v_{y}} & \frac{\partial F_{y}}{\partial v_{z}} & \frac{\partial F_{y}}{\partial \omega_{m}} \\ \frac{\partial F_{z}}{\partial v_{x}} & \frac{\partial F_{z}}{\partial v_{y}} & \frac{\partial F_{z}}{\partial v_{z}} & \frac{\partial F_{z}}{\partial \omega_{m}} \\ \frac{\partial T_{em}}{\partial v_{x}} & \frac{\partial T_{em}}{\partial v_{y}} & \frac{\partial T_{em}}{\partial v_{z}} & \frac{\partial T_{em}}{\partial \omega_{m}} \end{bmatrix} (41)$$

From (22) and (23) it can be noted that only the reflection term defined by (9) depends upon velocity. Substituting (23) and (22) into (41) yields

$$[\mathbf{D}] = lw \operatorname{Re} \sum_{m=-\infty}^{\infty} \sum_{n=-\infty}^{\infty} \frac{B_{mn}^{s}}{\kappa_{mn}} [\mathbf{M}_{mn}]$$
 (42)

where the  $4\times4$  matrix [ $\mathbf{M}_{mn}$ ] is

$$[\mathbf{M}_{mn}] = \begin{bmatrix} -j\xi_m \\ \kappa_{mn} \\ -jk_n \\ jP \end{bmatrix} \begin{bmatrix} \frac{\partial R_{mn}}{\partial v_x} & \frac{\partial R_{mn}}{\partial v_y} & \frac{\partial R_{mn}}{\partial v_z} & \frac{\partial R_{mn}}{\partial \omega_m} \end{bmatrix}$$
(43)

The derivatives of the reflection coefficient with respect to the velocity and angular velocity are

$$\frac{\partial R_{mn}}{\partial v_r} = j\xi_m [a_{mn} + \tau_{mn}(1 + \kappa_{mn}b_{mn})] / a_{mn}^2$$
(44)

$$\frac{\partial R_{mn}}{\partial v_y} = \kappa_{mn} [a_{mn} - 0.5 v_y b_{mn} \tau_{mn}] / a_{mn}^2$$
(45)

$$\frac{\partial R_{mn}}{\partial v} = jk_n[a_{mn} + \tau_{mn}(1 + \kappa_{mn}b_{mn})] / a_{mn}^2$$
(46)

$$\frac{\partial R_{mn}}{\partial \omega_m} = jP[a_{mn} + \tau_{mn}(1 + \kappa_{mn}b_{mn})] / a_{mn}^2$$
(47)

where  $a_{mn} = \left[\kappa_{mn}^2 + \gamma_{mn}^2 + 2\kappa_{mn}\beta_{mn} \coth(\beta_{mn}h)\right] / \mu_0 \sigma$  (48)

$$b_{mn} = \coth(\beta_{mn}h) / \beta_{mn} - h \operatorname{cosech}^{2}(\beta_{mn}h)$$
 (49)

It can be noted that as the form of (45) is different the damping matrix lacks symmetry.

## VI. DISCUSSION

In Fig. 2 the analytically calculated lift and drag force as a function of slip speed is compared with a finite element analysis (FEA) model. The parameters shown in Table I were used. The slip speed is defined as  $s=\omega_{\rm m}r_{\rm o}-v_x$ . In Fig. 3 the stiffness coefficients obtained from (34)-(36) are calculated using the values given in Table I. It can be noted that the stiffness coefficients  $k_{yy}$  is positive for increases in velocity, indicating stability, however  $k_{xx}$  and  $k_{zz}$  stiffness constants are both negative indicating instability along both the x and z axis. Further results are provided in [13]. The diagonal damping terms are shown in [13] to be all positive while off-diagonal damping term can lead to negative damping. For instance, the damping variation for  $D_{yx}$  and  $D_{xy}$  are shown in Fig. 4. For positive slip values  $D_{xy}$  provides negative damping while  $D_{yx}$ 

HP-6 4

has positive damping. This confirms that the cross coupling terms can create instability.

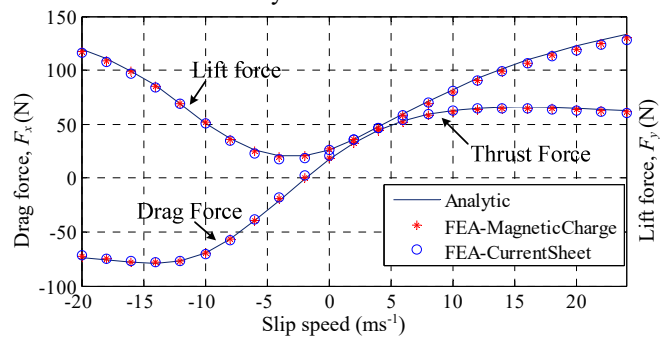


Fig. 2. Thrust/drag and lift force comparison between the presented analytic model and FEA models [13, 21] for  $(v_x, v_y, v_z) = (15, 0,0)$  ms<sup>-1</sup>.

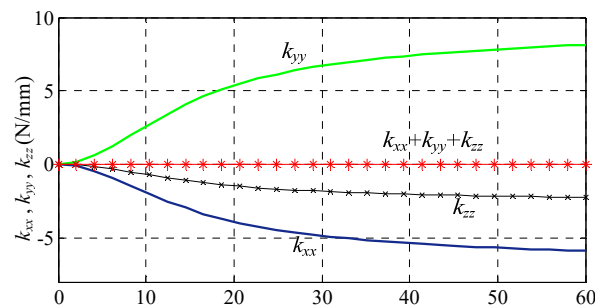


Fig. 3 The electrodynamic stiffness coefficients as a function of translational velocity for  $(\omega_e, \nu_y, \nu_z) = (0,0,0)$ .

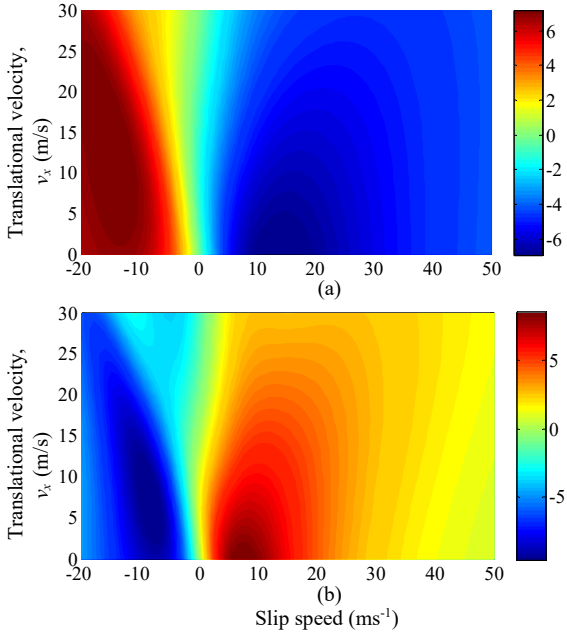


Fig. 4 (a) Damping coefficient  $D_{xy}$  and (b) damping coefficient  $D_{yx}$  all as a function of slip and translational velocity when  $(v_y, v_z)=(0,0)$ ms<sup>-1</sup>.

## VII. CONCLUSION

This paper presented the stiffness and damping equations in a form that enables the 3-D eddy current forces to be expressed in a linearized form. The presentation has been written in a general way in which different magnetic sources can be utilized. The approach presented here could be used to derive 3-D steady-state eddy current damping and stiffness matrices for other conducting plate geometries.

## REFERENCES

- Davis, L.C. and D.F. Wilkie, Analysis of motion of magnetic levitation systems: implications for high-speed vehicles. Jour. of Appl. Phy., 1971. 42(12): p. 4779-4793.
- Yoshida, K. and M. Takakura, Magnetic damping and stiffness coefficients in superconducting maglev system with sheet guideways. Electr. Eng. Japan, 1979. 99(12): p. 797-804.
- Langerhole, J., Electrodynamics of a magnetic levitation coil. Jour. Appl. Phy., 1973, 44: p. 2829-2837.
- Ebrahimian, M., M. Khodabakhsh, and G. Vossoughi, An analytical 3-D model fo calculating eddy-current damping force for a magnetic levitation system with permanent magnet. IEEE Trans. Magn., 2012. 48(9): p. 2472-2478.
- Sodano, H.A. and J. Bae, Eddy current damping in structures. The Shock and Vib. Digest, 2004. 36(6): p. 469-478.
- Nagaya, K., et al., Braking forces and damping coefficients of eddy current brakes consisting of cylindrical magnets and plate conductors of arbitrary shape. IEEE Trans. Magn., 1984. 20(6): p. 2136-2145.
- Paudel, N. and J.Z. Bird, Modeling the dynamic electromechanical suspension behavior of an electrodynamic eddy current maglev device. Progress in Electromagnetic Research B, 2013. 49: p. 1-30.
- 8. Paul, S., et al., 3-D eddy current torque modeling. IEEE Trans. Magn., 2014. **50**(2): p. 7022404.
- 9. Chen, C.-T., Linear System Theory and Design. 4th ed. 2012.
- Ooi, B.T. and M. Ivanes, Stiffness and damping matrices in free-body translational electromechanics. Elect. Mach. Power Sys., 1980. 5(1): p. 15-23.
- 11. Emson, C.R.I. and J. Simkin, *An optimal method for 3-D eddy currents*. IEEE Transactions on Magnetics, 1983. **19**(6): p. 2450-2452.
- Reitz, J.R. and L.C. Davis, Force on a rectangular coil moving above a conducting slab. Journal of Applied Physics, 1972. 43(4): p. 1547-1553.
- Paul, S., Three-dimensional steady state and transient eddy current modeling, in Elect. Comp. Eng. 2014, Univ. N.C. at Charlotte: Charlotte, NC.
- Earnshaw, S., On the nature of the molecular forces which regulate the constitution of the luminferous ether. Transactions Camb. Phil. Soc., 1842. 7: p. 97-112.
- 15. Kurz, S., J. Fetzer, and G. Lehner, *Three dimensional tranisent BEM-FEM coupled analysis of electrodynamic levitation problems.* IEEE Trans. on Magn., 1996. **32**(May): p. 1062-1065.
- Eastham, J.F. and E.R. Laithwaite, Linear induction motors as 'electromagnetic rivers'. Proceedings of the IEE, 1974. 121(10): p. 1099-1108
- Jefimenko, O.D., Electricity and Magnetism. 1966, New York: Meredith Publishing Co.
- Furlani, E.P., Permanent magnet and electromechnaical devices materials, analysis, and applications. 2001, San Diego: Academic Press.
- Moon, F.C., Superconducting Levitation: Applications to Bearings and Magnetic Transportation. 2004: WILEY-VCH Verlag GmbH & Co. KGaA.
- Paul, S., et al., Source field modeling in air using magnetic charge sheets. IEEE Trans. Mag., 2012. 48(11): p. 3879-3882.
- Bird, J. and T.A. Lipo, A 3D steady-state magnetic charge finite element model of an electrodynamic wheel. IEEE Trans. on Magn., 2008. 44(2): p. 253-265.